A Method for Disentangling El Niño-Mean State Interaction

Masahiro Watanabe[1] and Andrew T. Wittenberg[2]

1: Atmosphere and Ocean Research Institute, University of Tokyo, Kashiwa, Japan

2: NOAA Geophysical Fluid Dynamics Laboratory, Princeton, USA

Geophysical Research Letters

Submitted on April 13, 2012

Corresponding author:
M. Watanabe,
Atmosphere and Ocean Research Institute, University of Tokyo,
Kashiwa, Chiba 277-8568, Japan
(e-mail: hiro@aori.u-tokyo.ac.jp)

Abstract. The amplitude of the El Niño-Southern Oscillation (ENSO) is known to fluctuate in long records derived from observations and general circulation models (GCMs), even when driven by constant external forcings. This involves an interaction between the ENSO cycle and the background mean state, which affects the climatological precipitation over the eastern equatorial Pacific. The changes in climatological rainfall may be ascribed to several factors: changes in mean sea surface temperature (SST), changes in SST variability, and changes in the sensitivity of precipitation to SST. We propose a method to separate these effects in model ensembles. A case study with a single GCM demonstrates that the method works well, and suggests that each factor plays a role in changing mean precipitation. Applying the method to 16 pre-industrial control simulations archived in the Coupled Model Intercomparison Project phase 5 (CMIP5) reveals that the inter-model diversity in mean precipitation arises mostly from differences in the mean SST and atmospheric sensitivity to SST, rather than from differences in ENSO amplitude.

1. Introduction

Realistic simulation of the El Niño-Southern Oscillation (ENSO) phenomenon using coupled general circulation models (GCMs) is of great importance for predicting ENSO and evaluating its impact on global weather. The ability to simulate an ENSO with properties (amplitude, periodicity, spatial structure, phase asymmetry, etc) close to observations is a good test of a GCM. Despite improved ENSO simulations [*AchutaRao and Sperber 2006*], there was a large diversity in ENSO properties among the state of the art GCMs included in the Coupled Model Intercomparison Project phase 3 (CMIP3) [*Guilyardi et al. 2009, Vecchi & Wittenberg 2010*]. Errors in coupled feedback processes [*Collins et al. 2010; Philip et al. 2010; Lloyd et al. 2011*] are probably the major cause of the diversity of ENSO amplitudes among GCMs. However, the nonlinear nature of the coupled system makes it difficult to clarify how the error in a particular process affects ENSO and the mean state. In addition, intrinsic modulation can contribute to uncertainties in ENSO properties diagnosed from centennial and shorter records, such as the observed instrumental record and many climate simulations [*Wittenberg 2009*].

ENSO is known to interact with other phenomena on a variety of time scales: the annual cycle [*Jin et al. 1994; Guilyardi 2006*], atmospheric disturbances [*Vecchi et al. 2006; Jin et al. 2007*], and decadal variability [*An and Wang 2000; Choi et al. 2009*], all of which also affect the mean state. Here, we loosely define the 'mean state' as a time average spanning a period much longer thanENSO's interannual time scale. Changes in this background mean state can affect the growth rate and frequency of El Niño/La Niña, as has been clarified using a hierarchy of models [*Jin 1997; Fedorov and Philander 2001, Wittenberg 2002*]. ENSO can also feed back onto the mean state: El Niño exhibits a different spatial pattern of SSTAs than does La Niña, leading to a net warming of the eastern equatorial Pacific and cooling of the western Pacific during active ENSO epochs [*An and Jin 2004*]. Climate variables having a skewed probability distribution, such as precipitation, also exhibit mean state changes in response to changes in ENSO amplitude [*Watanabe et al. 2011*].

To improve understanding of ENSO in complex GCMs, it is necessary to devise useful metrics and methods for evaluating ENSO [*Guilyardi et al. 2012*]. Until now, there has been no simple method to isolate the ENSO feedback effect on changes in the tropical Pacific mean state. Here we propose such a method, using monthly time series of precipitation and SST from a sufficiently long simulation or an ensemble of simulations.

2. Method and model ensembles

The precipitation (P) over the tropical region depends nonlinearly on the underlying SST (T) [*Graham and Barnett 1987*]. The climatological mean precipitation $\bar{P}$ can be expressed as:

$$\begin{aligned}\bar{P} &= \int\int p(P,T)dPdT \\ &= \int\int p(T)p(P|T)dPdT \\ &= \int f(T)C(T)dT\end{aligned} \quad , \qquad (1)$$

where $p(X)$ denotes the probability distribution of X, f is the probability density function (PDF) of T, and $C(T)$ is the weighted-average composite of P with respect to T. In principle, the expression (1), hereafter referred to as the PDF method, holds exactly everywhere, regardless of the degree of correlation or causal linkage between *P* and *T*.

Given an ensemble of realizations (e.g. from different models, or different forcing scenarios), we may define references, denoted as $\overline{P}_0$, C_0, and f_0, and derive an equation for deviations from them, ( )';

$$\overline{P}-\overline{P}_0=\int f'C_0(T)dT+\int f_0C'(T)dT+\int f'C'(T)dT\ , \qquad (2)$$

where C_0 represents the typical shape of the precipitation composite and is obtained from the ensemble average of $C(T)$, i.e., $C_0 \equiv \langle C(T) \rangle$. At extreme values of *T*, the C_0 defined this way will be representative of only one or two models, but fortunately those extreme values of *T* are, by definition, rarely visited by the models. We have further assumed that wherever f=0, i.e. at those values of *T* not sampled by the ensemble member, *C* can be approximated as C_0, such that C'=0 at those values of *T*. The reference PDF f_0 is defined as $f_0 \equiv \left\langle f\left(T-\overline{T}+\langle \overline{T} \rangle\right)\right\rangle$, where $\overline{T}$ is the annual-mean climatology of *T* and $\langle \overline{T} \rangle$ is the ensemble average, to represent the plausible mean shape of the PDF while sharing the mean position with $\langle f \rangle$. $\overline{P}_0$ is expressed as $\overline{P}_0 \equiv \int f_0 C_0(T)dT$, so that the left hand side denotes the excess mean precipitation in a single ensemble member. The reference mean precipitation is slightly different from $\langle \overline{P} \rangle$, but the difference is about 5 % and negligible for the results presented in the next section. The first term on the right hand side of (2) captures the impact of a member's difference in SST PDF on $\overline{P}$, given the reference sensitivity of *P* to *T*. The second term, which captures the impact of a member's different sensitivity of P to T, given the reference PDF of T, is called the precipitation sensitivity feedback. The third term, which represents nonlinear impacts on $\bar{P}$, is small in most of the cases that we have tested. Here we apply (2) to the Niño 3 region (150° W-90° W, 5° S-5° N), so that the monthly time series of the Niño 3-averaged SST and precipitation are used for the analysis. The composite of P is computed using a Niño 3 SST bin width of 0.2 K.

A similar method has been used in cloud regime analysis, where cloud amounts are sorted by mid-tropospheric vertical velocity [*Bony et al. 2004*; *Bony and Dufresne 2005*]. In the present application, one has to be careful when interpreting the term involving f' since it includes not only the change in ENSO properties, but also biases or changes in mean SST and the seasonal cycle. The first term in (2) can therefore be decomposed as

$$\int f' C_0(T)dT = \int \left(f - \hat{f} \right) C_0(T)dT + \int \left(\hat{f} - f_0 \right) C_0(T)dT \quad , \qquad (3)$$

where $\hat{f}$ has the shape of f_0 but the mean $\bar{T}$ of f (Fig. 1). The first term on the right hand side represents the effect of the change in the shape of the temperature PDF, typically associated with an ENSO amplitude difference; we shall refer to it as the ENSO SSTA amplitude effect. The second term indicates the effect of the change in mean SST. While the difference in PDF shape, $f - \hat{f}$, is affected by the seasonal cycle, we confirmed that the results did not change much when the seasonal cycle was removed from T in advance (see discussion). Since the mean SST can be changed by either model biases or external forcing, the magnitude and impact of the mean SST effect will depend on the ensemble.

We demonstrate the evaluation of the ENSO SSTA amplitude effect with two types of model ensembles. One is a four-member ensemble from the Model for Interdisciplinary Research on Climate version 5 (MIROC5) [*Watanabe et al. 2010*]. Each member consists of a 100-year pre-industrial control run, with slightly different values of an entrainment parameter in the cumulus convection scheme. The ensemble spans a wide range of ENSO amplitudes from 0.61 to 1.63 K [*Watanabe et al. 2011*]. The other ensemble is the multi-model ensemble (MME) of the CMIP5, which is only partly available as of this writing [*Taylor et al. 2011*]. We use pre-industrial control runs from 16 different models (Table 1). The length of each CMIP5 run differs, but the statistics in (2)-(3) are calculated using all available data.

3. Results

Figure 2 summarizes the results of the PDF method applied to the MIROC5 ensemble. The ENSO amplitude systematically increases from one experiment (L575) to the other (L500), the latter showing a positively skewed SST PDF (Fig. 2a). The shape of $C(T)$ is similar for all the members, but the tail of intense precipitation extends as ENSO becomes stronger. The reconstruction of the Niño 3 mean precipitation, $\bar{P}_{\text{niño}}$, is successful by definition (black and purple bars in Fig. 2b). The decomposition of the total reconstruction into four components shows that in terms of the impact on mean precipitation, the change in ENSO SSTA amplitude can be as important as the change in mean SST. The change in precipitation sensitivity, which one might think of as being more directly affected by changes in convection parameters, here acts to counteract the change in $\overline{P}_{\text{niño}}$. This result is consistent with the arguments in *Watanabe et al.* [*2011*].

Before presenting the results for the CMIP5 MME, the ensemble-mean precipitation and its diversity are shown in Fig. 3. A preliminary analysis of the mean precipitation fields reveals that the pattern is not significantly improved over the CMIP3 MME [*N. Hirota, pers. comm.*], and still suffers from a double-ITCZ bias [*Bellucci et al. 2010*]. The spread among the 16 models (shading) indicates that the inter-model differences are especially large over the dry zones of the continents, subtropical oceans, and equatorial Pacific.

Unlike the previous example, the PDFs of T in CMIP5 models are shifted relative to each other, representing biases in mean SST (Fig. 4a). The shape of $C(T)$ is also different across the models, especially at higher values of SST (Fig. 4b). Figure 4c shows the reconstruction of $\overline{P}_{\text{niño}}$ for the 16 models, ordered following the ENSO amplitude. The diversity in $\overline{P}_{\text{niño}}$ exceeds 3 mm day^{-1} and is well reproduced by the PDF method. In contrast to the parameter ensemble shown in Fig. 2, the ENSO SSTA amplitude feedback, highly correlated with the ENSO amplitude (r=0.75), is much smaller in the MME. $\overline{P}_{\text{niño}}$ is roughly explained by the two effects in (2)-(3), which are not unique; a different shape of $C(T)$ revealed in Fig. 4b is critical in some models (*e.g.*, 2, 3, 11, 14, and 16) whereas the mean SST difference is critical in others (*e.g.*, 1, 4, 8, 12, and 13). Models showing that each term is very close to the ensemble mean (9 and 15) do not imply that they are "best," since the ensemble mean $\overline{P}_{\text{niño}}$ itself has a positive error of 0.27 mm day^{-1}.

4. Summary and discussion

We have shown that the PDF equations (2)-(3) work well in decomposing $\overline{P}_{\text{niño}}$ simulated in GCMs. The ENSO SSTA amplitude feedback works to increase $\overline{P}_{\text{niño}}$ due to asymmetry in the precipitation response to T. However, the relative importance of this term varies. In the parameter ensemble examined here from a single GCM, changes in $\overline{P}_{\text{niño}}$ are largely attributable to changes in both mean SST and SSTA amplitude. Given that $\overline{P}_{\text{niño}}$ can affect ENSO stability, a two-way feedback could conceivably contribute to low-frequency modulation of both ENSO and the mean state. In contrast, for the CMIP5 MME where models differ structurally in many aspects (dynamical core, physical parameterization scheme, and resolution), inter-model differences in $\overline{P}_{\text{niño}}$ are explained mainly by differences in mean SST, and by different sensitivities of precipitation to SST.

We have also tried defining *f* to be the PDF of the SSTA in (1). In this case, the first term in (2) cleanly represents just the ENSO SSTA amplitude influence on the mean precipitation. The second term then includes impacts of the change in mean SST on the precipitation response to SSTAs, which in the CMIP5 MME is larger than the impact of ENSO SSTA amplitude differences (Fig. 4). To estimate the SSTA amplitude impact on mean rainfall in an ensemble with large SST biases, it would be better to define *f* be the SSTA; however, the results are similar to those presented above. For example, the precipitation feedbacks (second term in (2)) in the CMIP5 MME are highly correlated (r=0.95) with the corresponding term when we use Niño3 SSTA to define *f*.

The PDF method has a potential for other applications. For example, one can use surface wind stresses instead of precipitation to understand causes of the diversity in the mean dynamical fields in the CMIP5 MME. Another application is to use a long, single-member integration [*e.g., Wittenberg 2009*]. The ensemble mean can be replaced by the long-term mean, while the deviation is defined using a particular epoch. The evaluation of MME can also be done by using observations to define f_0 and $C_0(T)$.

The PDF method could be extended to decompose T into $\bar{T}$, mean seasonal cycle, and anomalies. While the isolation of the seasonal cycle was not crucial in the present analysis, for some applications there might be an interaction among the mean state, seasonal cycle, and ENSO [*Guilyardi 2006*]. The asymmetric nature of ENSO can also modify $\bar{P}$ through changing $\bar{T}$ [*An and Jin 2004*]. Thus, our method should ultimately disentangle the impacts of changing variance and skewness of ENSO on the mean precipitation and SST.

Acknowledgments. MW is grateful to F.-F. Jin for stimulating discussion. Thanks are also due to M. Collins and J.-S. Kug for their encouragement. This work was supported by the Innovative Program of Climate Change Projection for the 21st Century from MEXT, Japan, and the Mitsui Environment Fund C-042.

References

AchutaRao, K. and K. Sperber (2006), ENSO simulations in coupled ocean-atmosphere models: Are the current models better? *Clim. Dyn.*, **27**, 1-15.

An, S.-I., and B. Wang (2000), Interdecadal change of the structure of the ENSO mode and its impact on the ENSO frequency. *J. Climate*, **13**, 2044-2055.

An, S.-I., and F.-F. Jin (2004), Nonlinearity and asymmetry of ENSO. *J. Climate*, **17**, 2399-2412.

Bellucci, A., S. Gualdi, and A. Navarra (2010), The double-ITCZ syndrome in coupled general circulation models: The role of large-scale vertical circulation regimes. *J. Climate*, **23**, 1127-1145.

Bony, S., J.-L. Dufresne, H. LeTreut, J.-J. Morcrette, and C. Senior (2004), On dynamic and thermodynamic components of cloud changes. *Clim. Dyn.*, **22**, 71-86.

Bony, S., and J. L. Dufresne (2005), Marine boundary layer clouds at the heart of tropical cloud feedback uncertainties in climate models. *Geophys. Res. Lett.*, **32**, L20806.

Choi, J., S.-I. An, B. Dewitte, and W. M. Hsieh (2009), Interactive feedback between the tropical Pacific decadal oscillation and ENSO in a coupled general circulation model. *J. Climate*, **22**, 6597-6611

Collins, M., and Coauthors (2011), The impact of global warming on the tropical Pacific Ocean and El Niño. *Nature Geo.*, **3**, 391-397.

Fedorov, A. V., and S. G. Philander (2001), A stability analysis of tropical ocean–atmosphere interactions: Bridging measurements and theory for El Niño. *J. Climate*, **14**, 3086-3101.

Graham, N. E., and T. P. Barnett (1987), Sea surface temperature, surface wind divergence, and convection over tropical oceans. *Science*, **238**, 657-659.

Guilyardi, E. (2006), El Niño–mean state–seasonal cycle interactions in a multi-model ensemble. *Clim. Dyn.*, **26**, 329-348.

Guilyardi, E., and Coauthors (2009), Understanding El Niño in ocean-atmosphere general circulation models: Progress and challenges. *Bull. Amer. Meteor. Soc.*, **90**, 325-240.

Guilyardi, E., and Coauthors (2012), A first look at ENSO in CMIP5. *CLIVAR exchanges*, submitted.

Jin, F.-F., J. D. Neelin, and M. Ghil (1994), El Niño on the devil's staircase: Annual subharmonic steps to chaos. Science, **264**, 70-72.

Jin, F. F. (1997), An equatorial ocean recharge paradigm for ENSO. Part II: A stripped-down coupled model. *J. Atmos. Sci.*, **54**, 830-847.

Jin, F.-F., L. Lin, L., A. Timmermann, and J. Zhao (2007), Ensemble-mean dynamics of the ENSO recharge oscillator under state-dependent stochastic forcing. *Geophys. Res. Lett.*, **34**, L03807.

Lloyd, J., E. Guilyardi, and J. Weller (2011), The role of atmosphere feedbacks during ENSO in the CMIP3 models. Part II: using AMIP runs to understand the heat flux feedback mechanisms. *Clim. Dyn.*, **37**, 1271-1292.

Meehl, G. A., and Coauthors (2007), Global climate projections. In *Climate Change 2007: The Physical Science Basis.* Eds. Solomon, S. et al., Cambridge Univ. Press.

Philip, S. Y., M. Collins, G. J. van Oldenborgh, and B. J. J. M. van den Hurk (2010), The role of atmosphere and ocean physical processes in ENSO in a perturbed physics coupled climate model. *Ocean Sci.*, **6**, 441-459.

Taylor, K. E., R. J. Stouffer, and G. A. Meehl (2011), An overview of CMIP5 and the experiment design. *Bull. Amer. Meteor. Soc.*, doi:10.1175/ BAMS-D-11-00094.1.

Vecchi, G. A., and A. T. Wittenberg (2010): El Niño and our future climate:

Where do we stand? Wiley Interdisciplinary Reviews: Climate Change, 1, 260-270. doi:10.1002/wcc.33

Vecchi, G. A., A. T. Wittenberg, and A. Rosati, (2006), Reassessing the role of stochastic forcing in the 1997–8 El Niño. *Geophys. Res. Lett.*, **33**, L01706.

Watanabe, M., and Coauthors (2010), Improved climate simulation by MIROC5: Mean states, variability, and climate sensitivity. *J. Climate*, **23**, 6312-6335.

Watanabe, M., M. Chikira, Y. Imada, and M. Kimoto (2011), Convective control of ENSO simulated in MIROC5. *J. Climate*, **24**, 543-562.

Wittenberg, A. T. (2002): ENSO response to altered climates. Ph. D. thesis, Princeton University. 475 pp.

Wittenberg, A. T. (2009), Are historical records sufficient to constrain ENSO simulations? *Geophys. Res. Lett.*, **36**, L12702.

Table and Figure Captions

Table 1: List of the CMIP5 models and the integration length of the pre-industrial control experiments.

Figure 1: Schematic of the SST PDF and its decomposition. $\hat{f}$ has the same shape as f_0, but the mean of the PDF follows that of f.

Figure 2: (a) PDFs of the Niño 3 SST anomalies (thin curves) and associated composites of the Niño 3 precipitation (thick curves, mm day^{-1}) in the four

experiments by MIROC5. The shading indicates std dev of the composite. (b) Reconstruction of the mean Niño 3 precipitation, the reference value subtracted, following Eq. (2). The reference values obtained from the GCMs (black bars) are also presented. The std dev of the Niño 3 SST anomaly ($\sigma_{\text{niño}}$, K) is shown by yellow circles. The names of the experiments follow *Watanabe et al. [2011]*.

Figure 3: Multi-model ensemble mean of $\bar{P}$ (contour, mm day^{-1}) and the inter-model spread scaled by the ensemble mean (shading, %) obtained from the pre-industrial control runs by 16 CMIP5 models.

Figure 4: As in Fig. 2 but for 16 pre-industrial runs by CMIP5 models. The model number, sorted by $\sigma_{\text{niño}}$, is listed in Table 1. The decomposition uses (2) and (3).

Table 1

Model no.	Model name	Integration years	Model no.	Model name	Integration years
1	GISS-E2-R	850	9	MIROC5	500
2	INM-CM4	450	10	MPI-ESM-LR	1000
3	MRI-CGCM3	200	11	HadGEM2-CC	240
4	CSIRO Mk-3.6	500	12	CNRM-CM5	850
5	GISS-E2-H	1106	13	CanESM2	996
6	IPSL-CM5A-LR	800	14	NorESM1-M	500
7	IPSL-CM5A-MR	300	15	GFDL-CM3	500
8	GFDL-ESM2G	500	16	GFDL-ESM2M	500

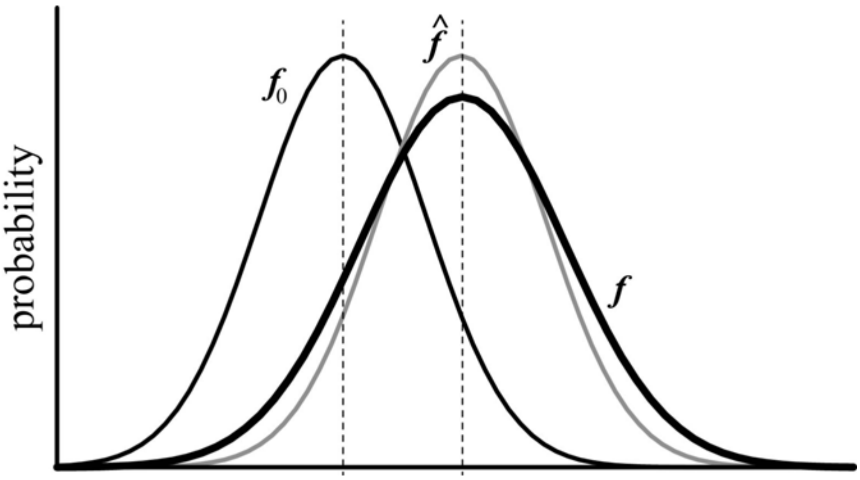

Figure 1

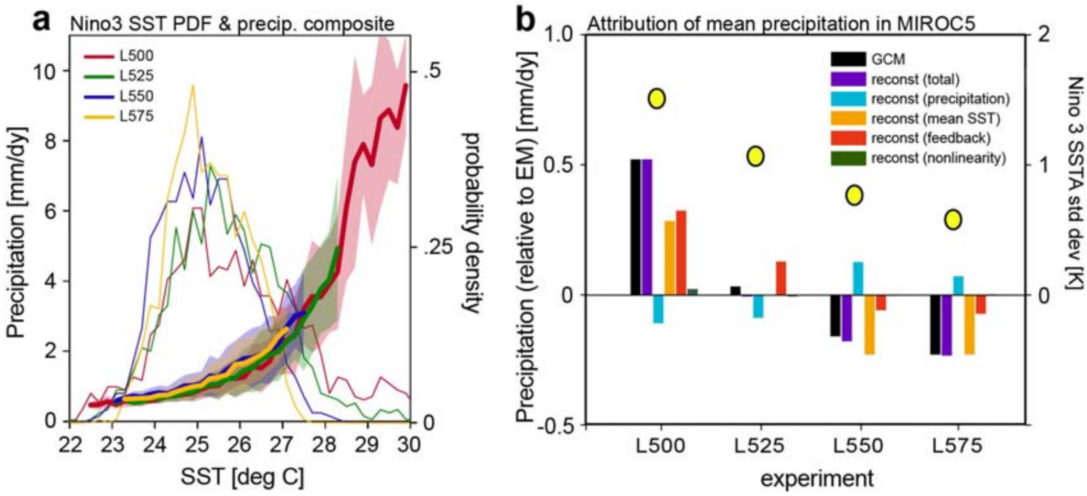

a
Nino3 SST PDF & precip. composite
L500
L525
L550
L575
Precipitation [mm/dy]
probability density
SST [deg C]
b
Attribution of mean precipitation in MIROC5
GCM
reconst (total)
reconst (precipitation)
reconst (mean SST)
reconst (feedback)
reconst (nonlinearity)
Precipitation (relative to EM) [mm/dy]
Nino 3 SSTA std dev [K]
L500
L525
L550
L575
experiment

Figure 2

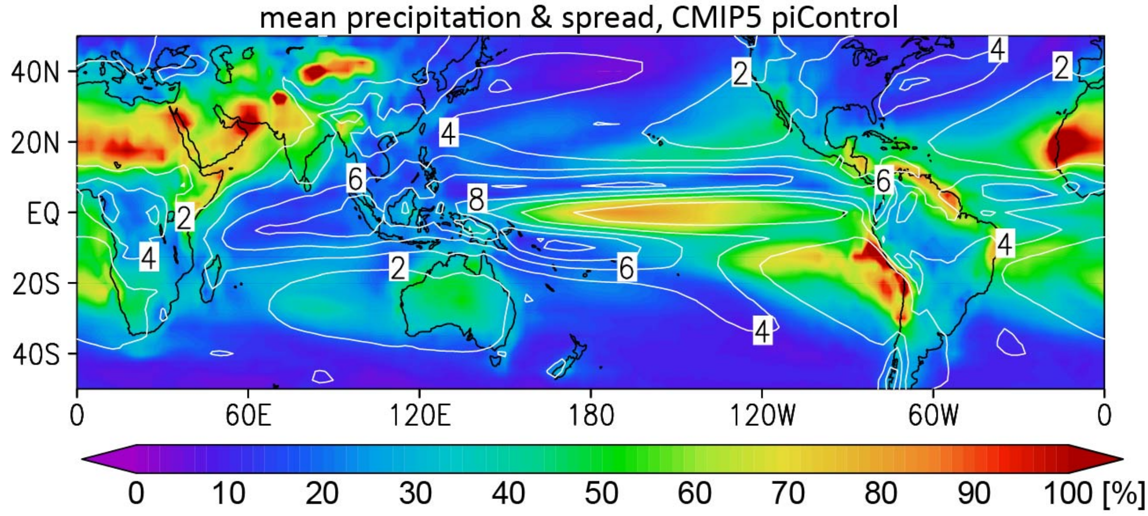
mean precipitation & spread, CMIP5 piControl
40N
20N
EQ
20S
40S
0
60E
120E
180
120W
60W
0
2
4
6
8
0
10
20
30
40
50
60
70
80
90
100 [%]

Figure 3

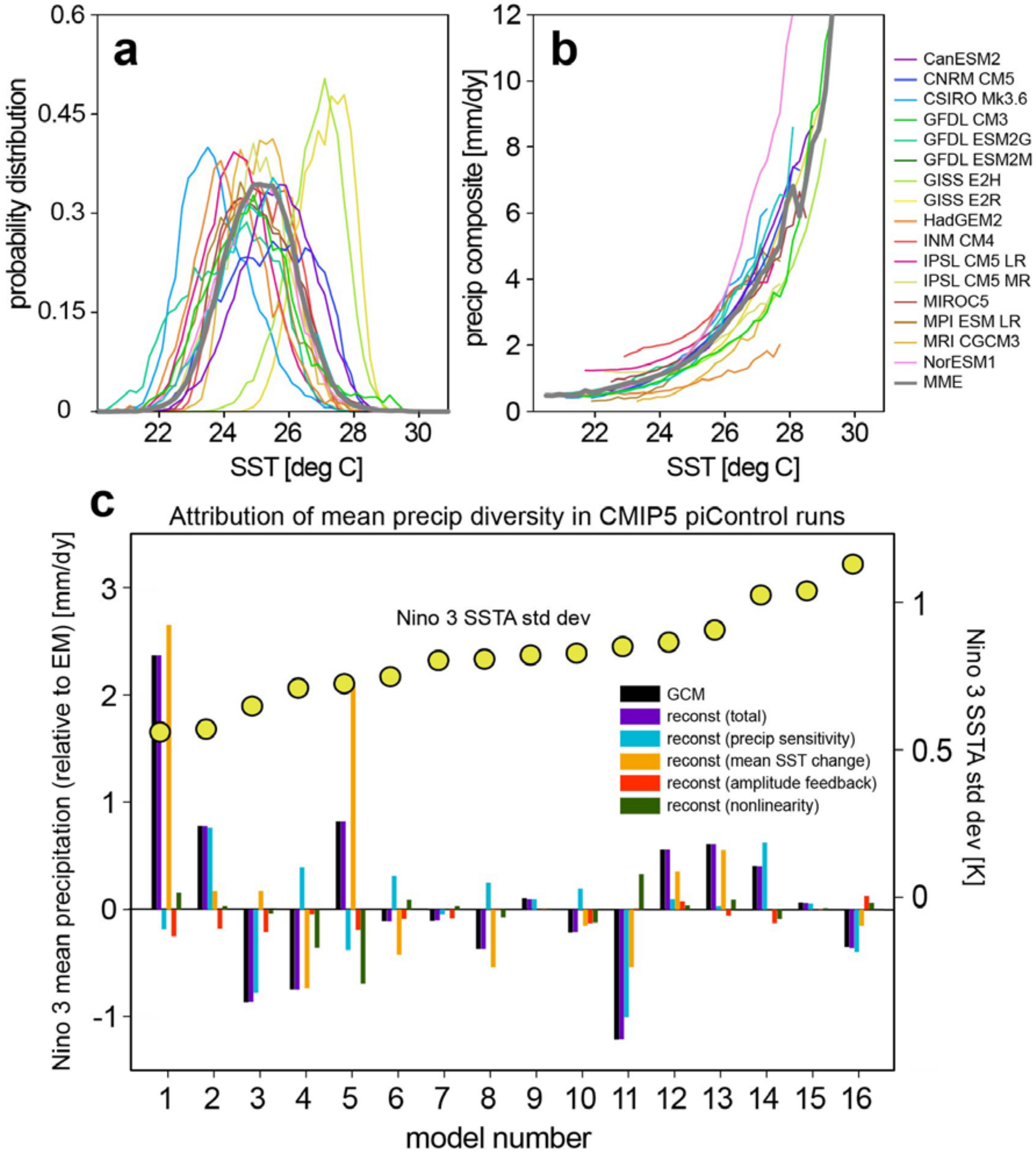
a
b
c
probability distribution
SST [deg C]
precip composite [mm/dy]
CanESM2
CNRM CM5
CSIRO Mk3.6
GFDL CM3
GFDL ESM2G
GFDL ESM2M
GISS E2H
GISS E2R
HadGEM2
INM CM4
IPSL CM5 LR
IPSL CM5 MR
MIROC5
MPI ESM LR
MRI CGCM3
NorESM1
MME
Attribution of mean precip diversity in CMIP5 piControl runs
Nino 3 SSTA std dev
GCM
reconst (total)
reconst (precip sensitivity)
reconst (mean SST change)
reconst (amplitude feedback)
reconst (nonlinearity)
Nino 3 mean precipitation (relative to EM) [mm/dy]
Nino 3 SSTA std dev [K]
model number

Figure 4